Available online at www.sciencedirect.com

ScienceDirect

Scripta Materialia 96 (2015) 13–16

Scripta MATERIALIA

www.elsevier.com/locate/scriptamat

Segregation of boron at prior austenite grain boundaries in a quenched martensitic steel studied by atom probe tomography

Y.J. Li,* D. Ponge,* P. Choi and D. Raabe

Max-Planck Institut für Eisenforschung, Max-Planck-Str. 1, D-40237 Düsseldorf, Germany

Received 16 July 2014; revised 19 September 2014; accepted 19 September 2014
Available online 4 November 2014

The distribution of B and other alloying elements (C, Cr, Mo) at prior austenite grain boundaries (PAGBs) and in the matrix was quantified by atom probe tomography in a quenched martensitic steel. B and Mo were observed to be segregated only at PAGBs and to be absent at martensite–martensite boundaries. C is segregated both at PAGBs and at martensite–martensite boundaries, whereas Cr is homogeneously distributed in the probed volume. Our results indicate that B undergoes a non-equilibrium segregation.

Keywords: Atom probe tomography; Martensitic steels; Grain boundary segregation; Prior austenite grain boundaries; Non-equilibrium segregation

Addition of a small amount of B (typically 3–30 wt ppm) to low-alloy steels can significantly enhance their hardenability [1]. The reason for such an improvement has been frequently attributed to segregation of B at (prior) austenite grain boundaries (PAGBs), which may reduce the grain boundary energy, thus preventing the austenite to ferrite transformation and rendering bainite or martensite formation more favorable [2,3]. Depending on heat treatment conditions, segregation of B at grain boundaries (GBs) can be of equilibrium and/or non-equilibrium type. Equilibrium segregation [4] is driven by the difference in free enthalpy of solute atoms in the matrix and at interfaces such as grain boundaries. Solute segregation at grain boundaries hence thermodynamically minimizes the overall free energy of the system. Its magnitude decreases with increasing temperature. Non-equilibrium segregation [5], on the other hand, mainly occurs upon cooling from high temperatures, during which supersaturated vacancies are induced in the matrix. These vacancies diffuse towards vacancy sinks such as grain boundaries. They may drag solute atoms with them, leading to the non-equilibrium segregation of solutes at GBs. Therefore, in such cases the magnitude of segregation depends on the austenitization temperature and the cooling rate [6–9]. It is widely accepted that B segregation at PAGBs during cooling is controlled by a non-equilibrium mechanism [2,6–18].

Segregation of B at PAGBs in martensitic steels has been studied by particle tracking autoradiography (PTA) [2,9,13,16,18], secondary ion mass spectrometry (SIMS) [9,18,19] and electron energy loss spectroscopy (EELS) [17]. These characterization techniques, except EELS, are advantageous for large-scale (up to several hundred micrometers) investigations, providing overviews of distributions of B at GBs and B-containing precipitates. However, they are not the most appropriate approaches for quantitative analyses. As a complementary technique atom probe tomography (APT) traces individual atoms at the atomic scale, and thus delivers precise information on solute distribution at GBs, in precipitates and in the matrix. An APT study of B distribution in a tempered martensitic steel is reported in Ref. [19]. While segregation of B at PAGBs in tempered steels was observed [19], it is still not clear whether B segregation at PAGBs occurs during cooling (non-equilibrium segregation) or during subsequent tempering (equilibrium segregation). Also it is unclear whether B segregates to martensite–martensite (M–M) boundaries and how other alloying elements may influence B segregation. To answer these questions, one needs to investigate as-quenched steel. Since PAGBs are hard to reveal by chemical etching and hard to distinguish from other types of GBs such as block, packet boundaries or lath boundaries in martensite when preparing APT samples by focused-ion-beam (FIB) milling, investigations of B segregation at PAGBs become more difficult in a quenched steel.

In the present work we apply APT to study segregation of B, C, Mo and Cr at PAGBs and other types of boundary in an as-quenched martensitic steel. The quenched microstructure contains various boundaries, such as PAGBs and the newly formed packet and block boundaries as well as the martensite lath boundaries. For simplicity the newly formed boundaries during cooling are referred to as M–M boundaries. Prior austenite grains (PAGs) were reconstructed from electron backscatter diffraction (EBSD) orientation maps. Subsequently, FIB milling was applied

* Corresponding authors. Tel.: +49 211 6792853; fax: +49 211 6792333; e-mail addresses: y.li@mpie.de; d.ponge@mpie.de

http://dx.doi.org/10.1016/j.scriptamat.2014.09.031
1359-6462/

for site-specific preparation of APT samples containing PAGBs. We found that B and Mo are segregated only at PAGBs and B is not detected in the matrix. Based on the APT results, the mechanism of B segregation is discussed.

The material studied in this work is a low-carbon steel (Fe–0.19C–0.35Si–1.20Mn–0.20Cr–0.50Mo–0.06Al–0.03Nb–0.03V–0.00124B in wt.% or Fe–0.88C–0.70Si–1.21Mn–0.21Cr–0.29Mo–0.12Al–0.02Nb–0.03V–0.012B in at.%). The steel was austenitized at 930 °C for 15 min followed by water quenching. The cooling rate at the APT sampling location was approximately 30 °C s^{-1} within the first 20 s of quenching from 930 °C. A software, developed by CEA-Grenoble, Laboratory of Innovation for New Energy Technologies and Nanomaterials, France, was applied for reconstructing the PAGs from EBSD data according to the orientation relationship (Kurdjumov–Sachs) between the martensite variants and their parent austenite grain (see details in Ref. [20]). Figure 1a shows the EBSD orientation map of the as-quenched steel containing various unidentified boundaries of PAGs, blocks, packets and martensite laths. The reconstructed results are shown in Figure 1b and c. Three PAGBs marked by the red arrows in Figure 1c are correlated with those shown in the SEM image in Figure 1d. The PAGB to be investigated by APT is marked as PAGB3. These results were used as references to locate the corresponding PAGBs in both SEM (Fig. 1d) and FIB secondary electron image. Next, site-specific preparation [21] of APT samples containing PAGBs was performed using a dual-beam FIB (FEI Helios NanoLab 600TM). A local electrode atom probe (LEAP) (LEAP 3000X HR™, Cameca Instruments) was employed to analyze the element distributions. The measurements were performed in voltage mode at 70 K. B ions were detected at 3.6 Da (B^{3+}), 5 Da and 5.5 Da (B^{2+}), and 10 Da and 11 Da (B^{+}) in the sample containing a PAGB. No molecular MoB ions were detected.

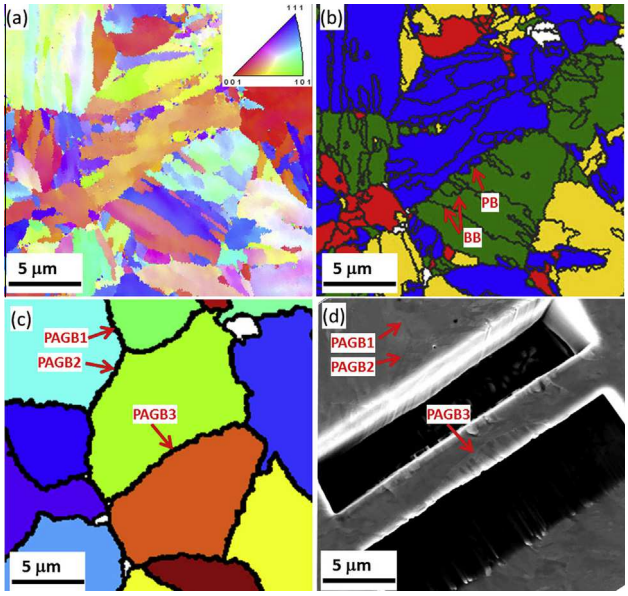

Fig. 1. Example of revealing PAGBs in an as-quenched martensitic steel. (a) Crystal orientation map measured using EBSD in SEM. (b) Reconstructed images displaying packet boundaries (PBs) and block boundaries (BBs). Colors represent packets with different orientations. The lines within a packet (a uniform color) are identified as block boundaries. Unindexed regions are marked by white color. (c) Reconstructed images showing only PAGs. The colors represent PAGs with different orientations. (d) SEM image marking three correlative PAGBs with those in (c) by red arrows. Two mill cuts were done to extract PAGB3. (For interpretation of the references to color in this figure legend, the reader is referred to the web version of this article.)

Figure 2 shows the atom maps of several selected solute species (B, Mo, C and Cr) in the as-quenched martensite. Results on other elements such as Nb and P (similar to Mo) and Si, Mn, Al and V (similar to Cr) will be presented elsewhere. Figure 2a reveals that B, C and Mo are strongly segregated to the PAGBs. The substitutional solute Cr is homogeneously distributed throughout the entire detected volume. Figure 2b shows the distribution of these atoms in the martensite matrix. The volume probed does not contain any PAGBs but two M–M boundaries. While no B is detected in the entire probed volume, C is observed to be segregated at the two M–M boundaries, which are almost parallel to each other and located at a distance of about 50 nm from each other. Interestingly, Mo and Cr are not observed to segregate at the M–M boundaries in this sample.

1-D concentration profiles of these elements within ROI1 (oval cross-sectional cylinder, Fig. 3a) along the arrow direction show a peak value of 2 at.% for B at the

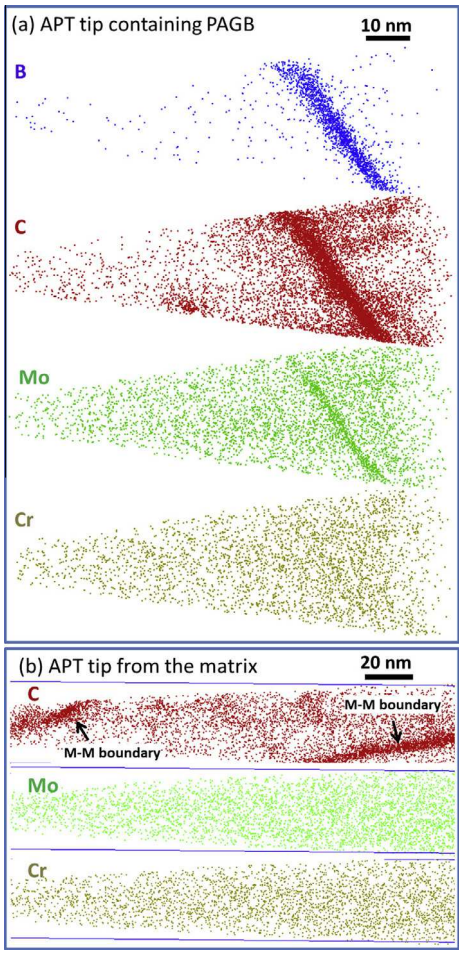

Fig. 2. 3-D atom maps of the as-quenched martensitic steel. (a) Distributions of atoms in the probed volume containing a PAGB. Significant segregation of B, C and Mo and no segregation of Cr at the PAGB. (b) Distributions of atoms in the martensite matrix containing two M–M boundaries with C segregation. Mo and Cr are homogeneously distributed.

PAGB (Fig. 3b), which is two orders of magnitude higher than the nominal value of 0.012 at.% (24 wt ppm B). C and Mo enrich at the PAGBs with concentrations 5–8 times higher than their nominal values. The concentration of Cr equals its corresponding nominal value (marked by an arrow in Fig. 3c) indicating no segregation at the PAGBs. Figure 4a shows the distribution of C, B and Mo in ROI2. This ROI provides a view into the PAGB plane. It can be seen that the three elements exist as individual solutes in the PAGB and form neither clusters nor carbides. However, it should be noted that this observation does not rule out the existence of B-containing precipitates in regions outside of the small APT sample.

It is known that the concentration of a solute species at grain boundaries measured by APT could be underestimated to a certain extent due to the local magnification effect [22]. In this case the Gibbs interfacial excess value Γ_X of solute X (atoms per grain boundary area) can be additionally used for the assessment of the degree of segregation. It should be noted that while the Γ_X may be influenced by the multiple-hit ions, for the present case the percentage of multiple-hit ions is only about 15%, thus systematic errors caused by the multiples should be excluded here. According to the method described in Ref. [23] the numbers of solutes N_B, N_C and N_{Mo} (vertical arrows in Fig. 4b) were determined for the grain boundary area contained in ROI1. The corresponding values for Γ_B, Γ_C and Γ_{Mo} determined by APT are 5.27, 15.76 and 1.43 atoms nm^{-2}, respectively.

Accurate analyses of solute distributions in the matrix were also done for ROI3 shown in Figure 3a. No B peaks were detected in the mass spectrum in ROI3, which means that the martensite matrix is virtually free of B. This result

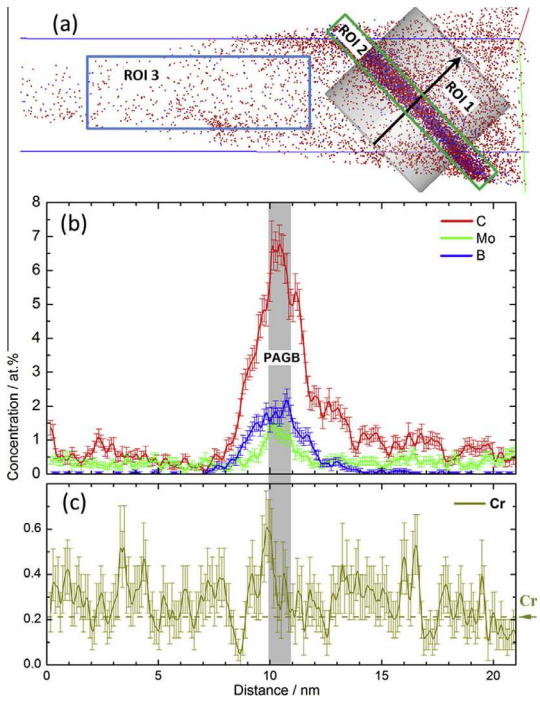

Fig. 3. (a) Three regions of interest (ROIs) are selected for further analysis of the distributions of various atoms. (b,c) 1-D concentration profiles within ROI1 along the direction marked by the black arrow in (a) for segregating atoms B, C and Mo and for homogeneously distributed atom Cr, respectively. The dotted line and arrow in (c) mark the nominal chemical composition of Cr.

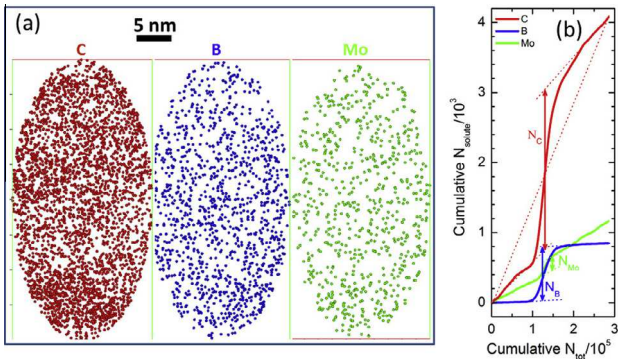

Fig. 4. (a) Distributions of C, B and Mo on the PAGB plane within ROI2 (5 nm thick slice with an oval cross-section shown in Fig. 3a). View direction parallel to the black arrow in Figure 3a. (b) Determination of grain boundary excess number of C, B and Mo from the APT analyses of ROI1 according to the method described in Ref. [23].

is consistent with the measurement shown in Figure 2b. The small amount of B atoms in the martensite shown in Figure 2a originates from the background noise signal. Unlike B, C and Mo are present in the martensite matrix.

The present work gives insights into the distribution of solute atoms in the matrix and at boundaries in an as-quenched martensitic steel. While C, B and Mo are essentially co-segregated at PAGBs, they show different individual segregation effects. C is segregated both at PAGBs and at the M–M boundaries. For the present material martensite transformation starts at 400 °C. The non-equilibrium segregation of C to the M–M boundaries can be excluded due to a low cooling rate in the temperature range <400 °C where only a mild vacancy concentration gradient is generated; thus, segregation of C at M–M boundaries should be of equilibrium type [24–26]. It is known that the diffusivity of carbon in martensite is sufficiently high and enables such segregation. Similar observation of carbon segregation during quenching was also reported in Ref. [27]. With respect to segregation of C at PAGBs, it may also occur through an interstitial diffusion mechanism.

Unlike C, B is only segregated at PAGBs. Segregation of B at M–M boundaries should not be expected, because in the present case all B atoms that were originally dissolved in the matrix have already been segregated at PAGBs during cooling before the martensite transformation starts. This result further indicates that segregation of B to PAGBs occurs by non-equilibrium mechanism. Although Mo atoms partially remain in the matrix after quenching and are thermodynamically prone to segregate to M–M boundaries as observed in a maraging stainless steel [28], segregation to M–M boundaries is not observed here (Fig. 2b). This means that the diffusion of Mo is too low to reach an interface trap and the possibility of Mo segregation to either PAGBs or M–M boundaries via an equilibrium mechanism can be eliminated. Thus, the observed segregation of Mo at the PAGB has probably occurred, similar to B, during cooling before the austenite to martensite transformation, i.e. via a non-equilibrium mechanism.

It has been observed that the significance of non-equilibrium segregation of a solute strongly depends on its binding energy with vacancies. The binding energies between a vacancy and B and Mo are about 0.48 and 0.31 eV [6], respectively, which fall into the range of ~0.3–0.6 eV for the occurrence of non-equilibrium grain boundary

segregation, as suggested by Xu [31]. In contrast, due to a low binding energy between Cr and a vacancy [32], non-equilibrium segregation at PAGBs does not occur for Cr. During cooling when the austenite reaches the martensite start temperature (400 °C for the present material), the martensitic reaction begins. Cr segregation to M–M boundaries is thermodynamically favored, similar to Mo, but it is kinetically limited due to its low diffusivity (diffusion length <1 nm at 400 °C for 1 h according to the diffusion coefficient given in Ref. [33]). This leads to a homogeneous distribution of Cr in the as-quenched martensite.

Due to the excellent synergistic effect of B and Mo on the hardenability of steels [2,29,30] the co-segregation behavior of B and Mo has been studied mainly for Ni-based superalloys using energy-dispersive X-ray spectroscopy [14] and 3-D APT [35,36] as well as for austenitic stainless steels using SIMS [7] and 1-D atom probe [34]. The current work reports a direct observation and the first quantitative analysis of segregation of Mo at PAGBs in an as-quenched martensitic steel. It has been suggested that Mo may promote non-equilibrium segregation of B at PAGBs by forming B–Mo complexes [14] because the binding energy of this type of complex is higher than that of a B–vacancy complex. In the present observation the measured Γ_B and Γ_{Mo} values show that the atomic density of B atoms is nearly four times that of Mo atoms at PAGBs. This result suggests that the formation of B–Mo complexes may not be the major mechanism of B segregation at PAGBs in the present as-quenched steel. The formation and diffusion of B–vacancy complexes is instead assumed to be the controlling mechanism. Investigations on a Mo-free steel are currently being conducted to further clarify the effect of Mo on B segregation.

In summary, the application of APT to PAGBs which were identified and reconstructed from EBSD data enabled the site-specific preparation and analysis of the associated segregation behavior. More specifically, we addressed the equilibrium and non-equilibrium segregation of B, Mo, C and Cr in an as-quenched martensitic steel. B and Mo are found to segregate at PAGBs via a non-equilibrium mechanism. Quantitative analyses of interfacial excess values indicate that the segregation of B occurs by forming mainly B–vacancy complexes. C is segregated to both PAGBs and M–M boundaries, whereas Cr is homogeneously distributed throughout the entire detected volume. These results demonstrate that APT is a powerful technique for precisely quantifying the distribution of alloying elements, which can deliver essential knowledge for both a fundamental understanding of grain boundary segregation, and for selecting the B and Mo content that optimizes the hardenability of low-carbon steels.

The research leading to these results has received funding from the European Union's Research Fund for Coal and Steel (RFCS) research programme under Grant Agreement No. [RFCS-CT-2012-00018]. The authors thank Mr. M. Green from Tata Steel Research and Development for providing the steel samples. We also thank Dr. H. Zhang from Max-Planck Institut für Eisenforschung for valuable discussions. Dr. I. Gutierrez, Mr. M. Green, Dr. W. Xu and Dr. I. Tolleneer are gratefully acknowledged for their scientific and technical support within the RFCS project.

[1] M. Ueno, K. Itoh, Tetsu-to-Hagané 74 (1988) 1073–1080.
[2] H. Asahi, ISIJ Int. 42 (2002) 1150–1155.
[3] S. Khare, K. Lee, H.K.D.H. Bhadeshia, Int. J. Mater. Res. 100 (2009) 1513–1520.
[4] D. McLean, Grain Boundaries in Metals, Oxford Univ. Press, London, 1957.
[5] K.T. Aust, R.E. Hanneman, P. Niessen, J.H. Westbrook, Acta Metall. 16 (1968) 291–302.
[6] R.G. Faulkner, Acta Metall. 35 (1987) 2905–2914.
[7] L. Karlsson, H. Nordén, H. Odelius, Acta Metall. 36 (1988) 1–12.
[8] X.L. He, Y.Y. Chu, J.J. Jonas, Acta Metall. 37 (1989) 147–161.
[9] D.J. Mun, E.J. Shin, K.C. Cho, J.S. Lee, Y.M. Koo, Metall. Mater. Trans. A 43 (2012) 1639–1648.
[10] J.D. Garnish, J.D.H. Hughes, J. Mater. Sci. 7 (1972) 7–13.
[11] T.M. Williams, A.M. Stoneham, D.R. Harries, Metal Sci. 10 (1976) 14–19.
[12] L. Karlsson, H.O. Andren, H. Norden, Scripta Metall. 16 (1982) 297–302.
[13] X.L. He, M. Djahazi, J.J. Jonas, J. Jackman, Acta Metall. 39 (1991) 2295–2308.
[14] S. Dumbill, R.M. Boothby, T.M. Williams, Mater. Sci. Technol. 7 (1991) 385–390.
[15] T. Sourmail, T. Okuda, J.E. Taylor, Scripta Mater. 50 (2004) 1271–1276.
[16] B. Hwang, D.W. Suh, S.J. Kim, Scripta Mater. 64 (2011) 1118–1120.
[17] G. Shigesato, T. Fujishiro, T. Hara, Mater. Sci. Eng. A 556 (2012) 358–365.
[18] S. Kim, Y. Kang, C. Lee, Mater. Sci. Eng. A 559 (2013) 178–186.
[19] J.B. Seol, N.S. Lim, B.H. Lee, L. Renaud, C.G. Park, Met. Mater. Int. 17 (2011) 413–416.
[20] C. Cayron, J. Appl. Crystallogr. 40 (2007) 1183–1188.
[21] K. Thompson, D. Lawrence, D.J. Larson, J.D. Olson, T.F. Kelly, B. Gorman, Ultramicroscopy 107 (2007) 131–139.
[22] M.K. Miller, M.G. Hetherington, Surface Sci. 246 (1991) 442–449.
[23] B.W. Krakauer, D.N. Seidman, Phys. Rev. B 48 (1993) 6724–6729.
[24] Y.J. Li, P. Choi, S. Goto, C. Borchers, D. Raabe, R. Kirchheim, Acta Mater. 60 (2012) 4005–4016.
[25] Y.J. Li, D. Raabe, M. Herbig, P. Choi, S. Goto, A. Kostka, H. Yarita, C. Borchers, R. Kirchheim, Phys. Rev. Lett. 113 (2014) 106104.
[26] M. Herbig, D. Raabe, Y.J. Li, P. Chio, S. Zeafferer, S. Goto, Phys. Rev. Lett. 112 (2014) 126103.
[27] L. Yuan, D. Ponge, J. Wittig, P. Choi, J.A. Jimnez, D. Raabe, Acta Mater. 60 (2012) 2790–2804.
[28] M. Thuvander, M. Andersson, K. Stiller, Ultramicroscopy 132 (2013) 265–270.
[29] T. Hara, H. Asahi, R. Uemori, H. Tamehiro, ISIJ Int. 44 (2004) 1431–1440.
[30] F. Han, B. Hwang, D.W. Suh, Z. Wang, D.L. Lee, S.J. Kim, Met. Mater. 14 (2008) 667–672.
[31] T.D. Xu, Scripta Metall. 37 (1997) 1643–1650.
[32] T.P.C. Klaver, D.J. Hepburn, G.J. Ackland, Phys. Rev. B 85 (2012) 174111.
[33] C.G. Lee, Y. Iijima, T. Hiratani, K. Hirano, Mater. Trans. JIM 31 (1990) 255–261.
[34] L. Karlsson, H. Nordén, J. Phys. Colloques 47 (1986) 257–262.
[35] D. Blavette, L. Letellier, P. Duval, M. Guttmann, Mater. Sci. Forum 207–209 (1996) 79–92.
[36] D. Tytko, P.P. Chio, J. Kloewer, A. Kostka, G. Inden, D. Raabe, Acta Mater. 60 (2012) 1731–1740.